Journal of Power Sources 229 (2013) 1–5

Contents lists available at SciVerse ScienceDirect

Journal of Power Sources

journal homepage: www.elsevier.com/locate/jpowsour

Short communication

Fe/V redox flow battery electrolyte investigation and optimization

Bin Li [a], Liyu Li [b], Wei Wang [a,*], Zimin Nie [a], Baowei Chen [a], Xiaoliang Wei [a], Qingtao Luo [a], Zhenguo Yang [b], Vincent Sprenkle [a]

[a] Pacific Northwest National Laboratory, P.O. Box 999, Richland, WA 99352, USA
[b] UniEnergy Technologies, LLC, 4333 Harbour Pointe Blvd. SW, Unit A, Mukilteo, WA 98275, USA

HIGHLIGHTS

- Electrolyte of Fe/V redox flow battery is thoroughly investigated and optimized.
- An electrolyte stable in a temperature range from −5 °C to 50 °C is identified.
- Cycling performance of the optimized electrolyte and low-cost membrane is reported.

ARTICLE INFO

Article history:
Received 5 September 2012
Received in revised form
27 November 2012
Accepted 28 November 2012
Available online 5 December 2012

Keywords:
Redox flow battery
Temperature stability
Electrolytes
Membrane
Separator

ABSTRACT

The recently invented iron (Fe)/vanadium (V) redox flow battery (IVB) system has attracted increasing attention because of its long-term cycling stability and low-cost membrane/separator. In this paper, we describe our extensive matrix study of factors such as electrolyte composition, state of charge (SOC), and temperature that influence the stability of electrolytes in both positive and negative half-cells. During the study, an optimized electrolyte that can be operated in a temperature range from −5 °C to 50 °C without precipitation is identified. Fe/V flow cells using the optimized electrolyte and low-cost separator exhibit satisfactory cycling performance at different temperatures. Efficiencies, capacities, and energy densities of flow batteries at various temperatures are studied.

1. Introduction

With the increasing need to seamlessly integrate renewable energy with the current electricity grid, energy-storage systems must play a more prominent role in bridging the gap between current technologies and a clean sustainable future in grid reliability and utilization [1]. Among the most promising energy-storage technologies are redox flow batteries (RFB) [2,3], which capitalize on reactions of two redox couples to fulfill the reversible conversion between electrical energy and chemical energy. With energy-bearing liquid electrolytes stored externally while the redox reaction proceeds in the electrode compartment, the most prominent advantage of RFBs compared to solid-state secondary battery systems is its ability to independently tailor the energy capacity and the power output. This distinct advantage allows critical latitude for designers to size RFBs for a wide spectrum of power and energy-storage applications, ranging from utility-scale storage (at MWh levels) such as energy wholesale service, to end-user applications (at kWh levels) such as home power backup. In addition, undesirable electrode processes are eliminated, especially the mechanical or structural stresses that accompany physical or chemical changes during cycling. Eliminating these stresses results in a potentially longer service life. Other attractive features of flow batteries include quick response, low self-discharge, and tolerance to over-charge and over-discharge, etc.

Regardless of its unique mechanism and compelling potentials and despite continuous research and development efforts over the last decade or so, RFBs have achieved a very limited market presence to date. Among the various factors that have hindered commercialization of RFBs, high cost probably is the most significant deterrent. For example, the all-vanadium redox flow battery (VRB) demands expensive perfluorinated polymer membrane (Nafion®), which accounts over 40% of the stack cost. [4] In addition, the long-term operational stability of VRBs is far from certain.

* Corresponding author. Tel.: +1 509 372 4097; fax: +1 509 375 2186.
E-mail address: wei.wang@pnnl.gov (W. Wang).

0378-7753/$ – see front matter © 2012 Elsevier B.V. All rights reserved.
http://dx.doi.org/10.1016/j.jpowsour.2012.11.119

VRBs often suffer from constant capacity decay as cycling proceeds [5,6], and iron/chromium redox flow batteries (ICBs) have a gas evolution issue [7,8]. Recently, Wang and co-workers at Pacific Northwest National Laboratory invented the Fe/V redox flow battery (IVB) system [9,10], which is based on reactions between Fe^{2+}/Fe^{3+} and V^{2+}/V^{3+} redox couples using mixed reactant solutions. The Gen-1 IVB employs pure hydrochloric acid (HCl) as the supporting electrolyte, which has demonstrated stable cycling with an energy efficiency of ~80% at room temperature using a Nafion® 212 membrane (N212) [9]. With a mixed-acid supporting electrolyte of sulfuric acid and hydrochloric acid, a 25% improvement in the discharge energy density was achieved with the Gen-2 IVB compared with the Gen-1 IVB [10]. The electrochemical performance of an IVB system has demonstrated successful capitalization of the combined benefits of both Fe/Cr and VRB flow battery systems while circumventing their intrinsic issues. In contrast with a Fe/Cr flow battery, stable electrochemical cycling with an energy efficiency of ~80% was achieved at room temperature without any catalyst loading. No hydrogen evolution was observed because of the considerably higher working potential of V^{2+}/V^{3+} (−0.25 V) on the negative electrode compared to the working potential of Cr^{2+}/Cr^{3+} (−0.41 V) and the replacement of oxygen evolution with the V^{4+}/V^{5+} redox reaction as the over-charge protection at the positive electrode. The lower potential of the Fe^{2+}/Fe^{3+} couple at the positive electrode of the Fe/V cell also reduces its corrosive strength compared to the VRB, allowing less expensive membranes to be employed, thus reducing the stack cost significantly.

In an RFB system, the electrolyte is of critical importance, which not only dictates the system energy density but also the stable operational window in terms of temperature and SOC range. Despite the pioneering work in the IVB system, its electrolyte has not been thoroughly studied. Further systematic investigation of the electrolyte was thus warranted to establish the correlation between composition and stability. In response, we conducted an extensive study with a focus on improving the stability of the IVB mixed-acid electrolyte in particular and different factors that affect the stability of the electrolyte (e.g., SOC, temperature, supporting electrolyte H_2SO_4 and HCl ratio, etc.). Our exhaustive study on the composition and stability relationship also identified an electrolyte composition that expanded the temperature stability range to from −5 °C to 50 °C as compared with the Gen-2 IVB electrolyte, further improving its ability to be used in different areas of the world with widely different climates.

2. Experimental

The setup of flow cells is described in detail in a previous report [9]. The flow cells consisted of two graphite-felt electrodes, two gold-coated copper current collectors, two polytetrafluorethylene (PTFE) gaskets, and a membrane (N212 or Daramic microporous separators). Before cell setup, graphite felts were annealed in air at 400 °C for 6 h to improve electrochemical activity and hydrophilic characteristics. Electrochemical performance of the Fe/V flow battery was carried out using a potentiostat/galvanostat (Arbin Instrument, USA) to provide a constant-current. The single cell was connected to two glass reservoirs containing balanced 50 mL "catholytes" and 50 mL "anolytes", respectively. Electrolytes were pumped at a flow rate of 20 mL min^{-1} while controlled by a peristaltic pump. The two reservoirs were both purged with nitrogen gas and then sealed prior to the electrochemical tests to minimize oxidation of the active species.

The original electrolytes contained 1.5 M Fe^{2+} ions and 1.5 M VO^{2+} ions (Fe^{2+}/V^{4+}) with various concentrations of proton, Cl^{-1}, and $SO_4{}^{2-}$ ions corresponding to solutions at the positive half-cell side with 0% SOC. The electrolytes were prepared by dissolving $FeSO_4$ or $FeCl_2$, $VOSO_4$ or $VOCl_2$ in deionized water. The highly conductive proton ions in aqueous solutions were sourced from hydrochloride acid or sulfuric acid. The Fe^{3+}/V^{4+} solutions representing the 100% SOC electrolyte at the positive half-cell and Fe^{2+}/V^{3+} solutions corresponding to 0% SOC electrolyte at the negative half-cell in actual IVB were obtained by charging the original Fe^{2+}/V^{4+} solutions on both sides using flow cells with N212 membranes to an upper voltage limit of 0.55 V at a low current density of 20 mA cm^{-2}. The upper voltage limit of 0.55 V is chosen so that the Fe^{2+}/V^{4+} solution at negative half-cell will only be reduced to Fe^{2+}/V^{3+} instead of Fe^{2+}/V^{2+} due to the much higher potential of V^{4+}/V^{3+} than that of V^{3+}/V^{2+}. The resultant solutions at the positive side and the negative side corresponding to Fe^{3+}/V^{4+} and Fe^{2+}/V^{3+} solutions, respectively.

Three kinds of solutions (Fe^{2+}/V^{4+}, Fe^{2+}/V^{3+}, and Fe^{3+}/V^{4+}) for each composition were put in different temperature-controlled baths in the temperature range from −10 °C to 50 °C. The samples were kept static without any agitation and were monitored daily by eye for precipitation. Precipitation was analyzed by X-ray diffraction (XRD) (Philips Xpert X-Ray Diffractometer, Germany). Because of the easy oxidation of V^{2+} ions, the stability of Fe^{2+}/V^{2+} solutions representing the 100% SOC electrolyte at the negative half-cell were studied after obtaining the optimized electrolytes based on the stability results of the three different solutions identified above. The electrolytes were deemed stable if no precipitate was observed after residing 10 days at a specific temperature. In addition to stability, electrolyte conductivity is another factor to be considered in the selection of electrolytes, which could significantly affect the energy efficiency of a flow cell. The conductivity of electrolytes was measured using a Conductivity Benchtop instrument (Orion 3 STARS, Thermo Scientific, USA). Among them, the most stable and conductive electrolyte and the microporous separator was used for electrochemical cycling performance test using a flow cell at a constant current density of 50 mA cm^{-2} within the voltage window between 1.35 V and 0.4 V. Electrochemical performance of the Fe/V mixed acid flow battery also was tested at different temperatures inside an environmental chamber (ESPEC, USA).

3. Results and discussions

In this study, the active materials concentration was fixed at 1.5 M for both iron and vanadium, as previously reported [10]. The composition−stability relationship was systematically studied in terms of the temperature, SOC, and ratio between $SO_4{}^{2-}$ and Cl^- concentration. For the original solutions, the Fe^{2+} and VO^{2+} ions were sourced from sulfates and/or chlorides as mentioned in the experimental section, from which the electrolytes with different compositions were selectively prepared. In actual solutions, the weak ionization of $[HSO_4]^-$ has a significant influence on the solution conductivity, which, however, was not considered for the preparations of solutions for simplicity. For the original solutions (Fe^{2+}/V^{4+}) corresponding to solutions with 0% SOC at the positive side, the relationship among all ions in Fe^{2+}/V^{4+} solutions can be described as follows according to the electrical neutrality of solutions:

$$[SO_4]^{2-} = \frac{6 - [Cl^-] + [H^+]}{2} \quad (1)$$

Because the concentration of sulfate ions $[SO_4]^{2-}$ can be determined from the concentrations of chlorine ions ($[Cl^-]$) and hydrogen ions ($[H^+]$), the experiment about solution stability involved varying $[Cl^-]$ and $[H^+]$, which are two independent parameters. The concentrations of apparent hydrogen ions (without considering the weak ionization of $[HSO_4{}^-]$) was changed successively from 2.5

to 4.5 M at 0.5 M intervals, and the concentrations of chlorine ions were varied from 4.5 to 8.5 M in the same fashion.

The actual experimental stability data of the Fe^{2+}/V^{4+} solutions are plotted in Fig. 1 using circle symbols, where the region labeled with Y means stable and N means unstable. Based on experimental data, the corresponding Fe^{3+}/V^{4+} and Fe^{2+}/V^{3+} solutions representing the 100% SOC positive electrolyte and 0% SOC negative electrolyte, respectively, are more stable than the original Fe^{2+}/V^{4+} solutions standing for the 0% SOC positive electrolyte. No apparent precipitation was observed for the Fe^{3+}/V^{4+} solutions and Fe^{2+}/V^{3+} solutions in the temperature range from −10 °C to 50 °C over a 10-day period. For Fe^{2+}/V^{4+} solutions, although the electrolyte is stable at room temperature and 50 °C, green crystal-like precipitates were observed for certain compositions when the temperature was decreased to 0 °C and/or −10 °C. All precipitates were filtered, dried, and subsequently identified to be $FeCl_2$ by XRD (as shown in Fig. 2). Therefore, the instability of Fe^{2+}/V^{4+} solutions

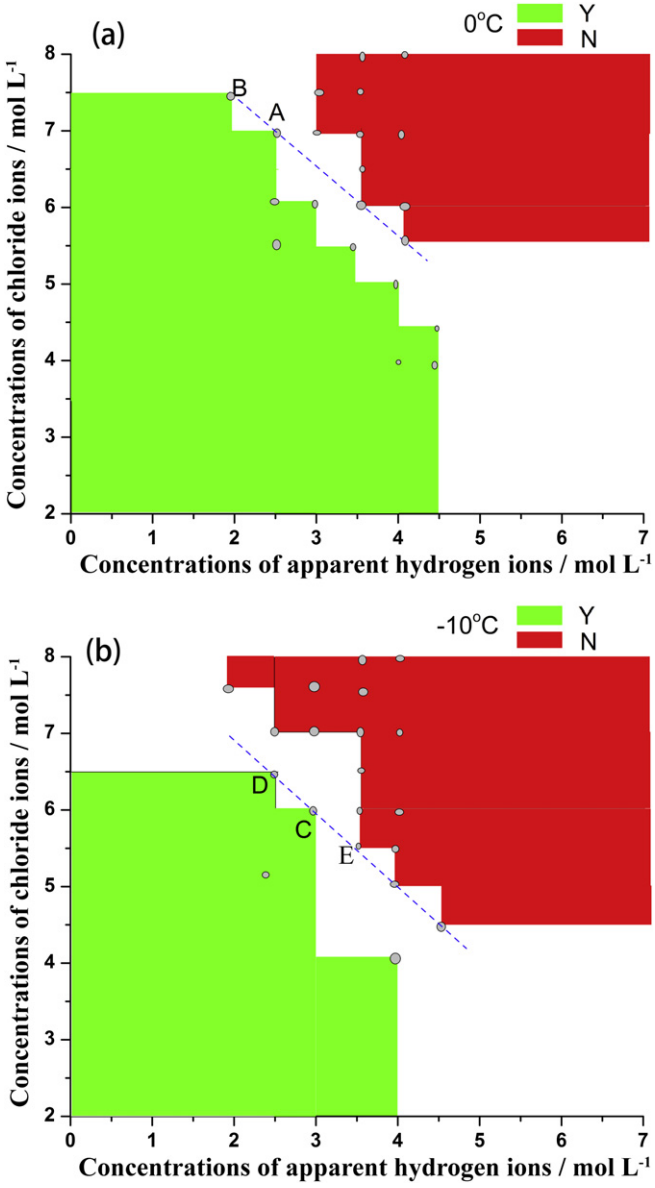

Fig. 1. Fe^{2+}/V^{4+} electrolyte stability with respect to concentrations of apparant hydrogen and chloride ions at (a) 0 °C and (b) −10 °C; Y and N represent stable and unstable solutions, respectively.

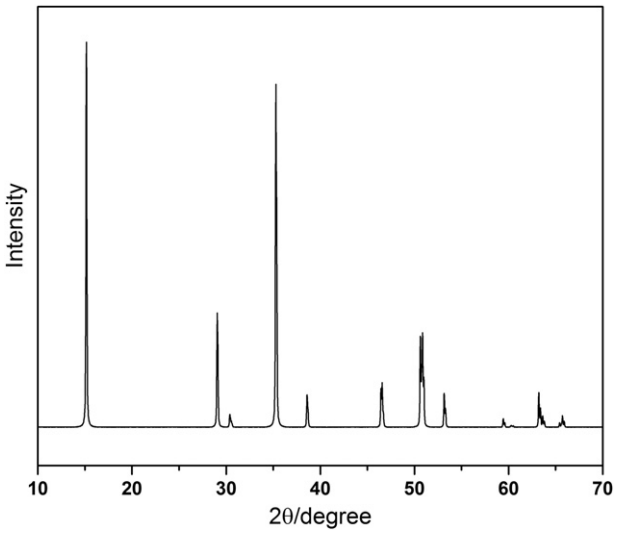

Fig. 2. XRD patterns of the green, crystal-like precipitates.

is attributed to decreasing solubility of $FeCl_2$ at lower temperatures. For the solutions containing $FeCl_2$, the dissociation reaction can be written as follows:

$$FeCl_2(s) \leftrightarrow Fe^{2+} + 2Cl^- \quad (2)$$

According to this equilibrium, the solubility product K can be described as:

$$K = a_{cl}[Cl^-]^2 a_{Fe}[Fe^{2+}] \quad (3)$$

where a_{Cl} is the activity coefficient of chlorine ions, and a_{Fe} is the activity coefficient of Fe^{2+}.

In very dilute solutions, activities can be taken as practically equal to the concentrations. Nevertheless, in the moderate concentrations of salts (1.5 M Fe^{2+} in this study), the activity coefficient is less than 1 [11]. According to Equation (2), the solubility of $FeCl_2$ decreases with increasing concentrations of chlorine ions with constant concentrations of apparent hydrogen ions, which agrees well with experimental observations as shown in Fig. 1. For example, at −10 °C and 0 °C, obvious precipitates (i.e., $FeCl_2$) were not found until the concentrations of chlorine ions reached 6.5 M and 7.0 M, respectively, at 3.0 M apparent hydrogen ions. Similarly, $FeCl_2$ was found to have a greater tendency to precipitate as the concentration of hydrogen ions increased while fixing the concentrations of chlorine ions, suggesting that the enhancement of hydrogen ions may improve the activity coefficients of Fe^{2+} or Cl^- or both ions (a_{Fe} and a_{Cl}). Hence the ionic concentration (and therefore the solubility) must decrease to maintain the solubility product constant [11]. As a result, reduction in both the chlorine ion and hydrogen ion concentrations resulted in an improvement of solution stability. Corroborated with this argument, the Fe^{2+}/V^{3+} solution is more stable than the original Fe^{2+}/V^{4+} solutions due to the reduction of proton concentration after the balance. According to the above tendency of $FeCl_2$ solubility in Fe^{2+}/V^{4+} solutions, the stability of the Fe^{2+}/V^{4+} electrolyte at 0 °C and −10 °C were expanded to a wider ranges of $[H^+]$ and $[Cl^-]$ based on the experimental data (marked with circles) as shown in Fig. 1. The compositions located in red zones are unstable in contrast to the stable electrolyte in green zones.

In actual solutions, a large portion of sulfur is present in the form of $[HSO_4^-]$ ions because of weak ionization of HSO_4^-

($K_2 = 1.2 \times 10^{-2}$ mol L^{-1}). The conductivities of the different ions in aqueous solutions are reported as follows [12]:

$$H^+ >> Cl^- > HSO_4^- \quad (4)$$

Accordingly, the increase of free hydrogen ions plays a more prominent role in the improvement of electrolyte conductivity. As shown in Fig. 1(a) and (b), the compositions along the dashed lines have similar free hydrogen ion concentrations if the calculation is based on the ionization constant of [HSO_4^-]. For example, as shown in Fig. 1(b), the concentrations of free hydrogen ions for the compositions at points D, C, and E along the dashed lines were calculated to be 1.5079 M, 1.5118 M, and 1.5196 M, respectively, showing that the concentrations of free hydrogen ions slightly increase with increasing concentrations of apparent hydrogen ions in the dashed lines. However, it was accompanied by a reduction in the concentration of chlorine ions. Therefore, the maximum conductivity exists for the electrolyte compositions that fall along the dashed lines of Fig. 1(b). Conductivities for these electrolytes were measured using the Conductivity Benchtop instrument. The conductivity data are shown in Fig. 3. The electrolytes with different compositions exhibited conductivity values in the close range of 148–156 S m^{-1}. In particular, the composition at Point C (1.5 M $FeCl_2$–1.5 M $VOSO_4$–3.0 M HCl) showed a slightly higher conductivity. We suspect that the compositions in the zones (in Fig. 1) below the dashed line exhibited lower conductivity than those at the dashed lines because of the decrease in the concentrations of chlorine and hydrogen ions. Therefore, the optimized electrolytes that can be obtained are summarized below:

1. At 0 °C, the stable solutions with highest conductivities are shown at Point A or Point B.
2. At −10 °C, the stable solutions with highest conductivities are shown at Point C or Point D.

As shown in Fig. 3, the composition at Point C (1.5 M $FeCl_2$–1.5 M $VOSO_4$–3.0 M HCl) can be stabilized at −10 °C and exhibited the highest conductivity. Hence, based on this particular composition, the solutions containing Fe^{2+} and V^{2+} corresponding to 100% SOC at the negative side were prepared by the charging process and transferred into several sealed reservoirs in a nitrogen-filled glove box. These reservoirs were put into temperature-controlled baths at different temperatures ranging from −10 °C to 50 °C. Purple-colored precipitates were observed within 10 days for the samples held at −10 °C. Based on the purple color, we believe the precipitates are vanadium(II). Nevertheless, no apparent precipitates were observed at −5 °C, room temperature, and 40 °C. Therefore, the electrolyte composed of 1.5 M $FeCl_2$–1.5 M $VOSO_4$–3.0 M HCl was considered to be the most stable solution in the temperature range from −5 °C to 50 °C, and it also exhibited the best conductivity.

IVBs provide much more freedom in the choice and development of alternative membranes due to the absence of highly oxidative V^{5+} ions [13]. Thus, a commercially available low-cost polyethylene microporous separator was employed in the electrochemical cyclic study. We then tested the electrochemical cycling performance of the 1.5 M $FeCl_2$–1.5 M $VOSO_4$–3.0 M HCl electrolyte in a flow cell using the microporous separator as the membrane. The cycling performance of the 1.5 M $FeCl_2$–1.5 M $VOSO_4$–3.0 M HCl electrolyte was tested at different temperatures inside an environmental chamber as shown in Fig. 4(a). As the temperature

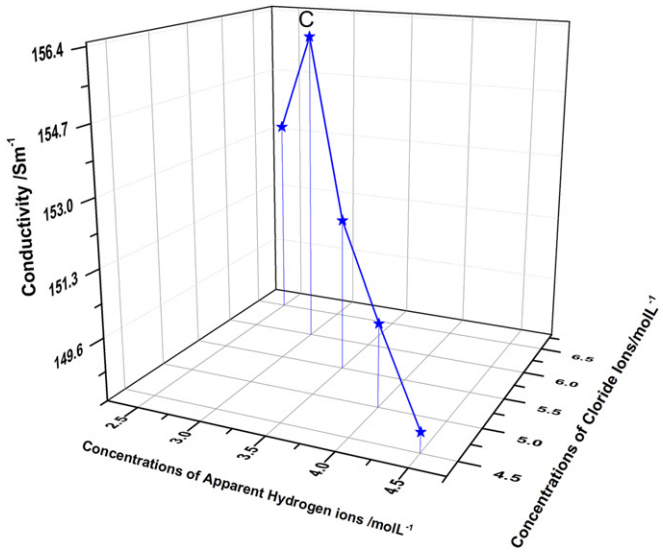

Fig. 3. Conductivities of the compositions along the dashed line in Fig. 1(b).

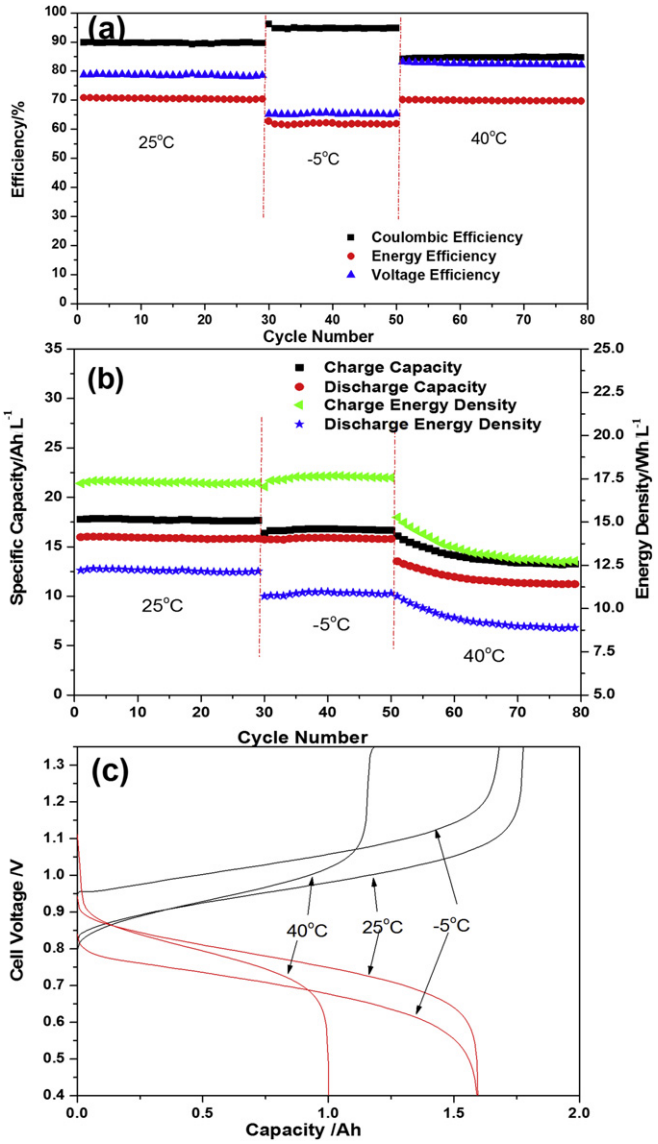

Fig. 4. Electrochemical performance of Fe/V RFBs with optimized electrolytes using a polyethylene microporous separator as the membrane at −5 °C, 25 °C, and 40 °C. (a) Efficiencies, (b) Capacities, and energy densities variety as a function of the cycle number. (c) Cell-voltage profile with respect to capacity during a typical charge/discharge process.

increased from −5 °C to 40 °C, the coulombic efficiency decreased from 95% to 85% while the voltage efficiency values increased from 65% to 83%. We attribute the decrease in coulombic efficiency to the amplified crossover of active species across the porous separator, while the increase in voltage efficiency resulted from the enhanced electrode reactions and conductivity of electrolytes. The lowest energy-efficiency value of the flow cells was 62% at −5 °C; similar energy-efficiency values of 70% were observed at both room temperature and 40 °C. Compared with the previously reported Fe/V cells with IEMs (N212), at the same temperature, the cells exhibited similar voltage-efficiency values even though the thickness of the microporous separator (450 μm) was much larger than that of the N212 used previously (50 μm), and the proton concentration in this study decreased by 0.8 M. These results indicate that all the ions (cations and anions) could pass through the separators from one side to the other during the charging/discharging process because of the microporous structures. This finding is completely different from the cells using IEMs (Nafion) in which conductivity through membranes mainly is accomplished by proton diffusion. However, because of its large pore size (around 150 nm), more severe reactant crossover through separators leads to lower coulombic-efficiency values for the separators.

Corresponding to the efficiency behavior at different temperatures, a higher capacity and energy density loss over cycling was observed at a higher temperature (40 °C) because of the elevated crossover through the separator, which corresponds to the lower coulombic-efficiency values as shown in Fig. 4(b). Nevertheless, at lower temperatures (i.e., room temperature and −5 °C), the cells exhibit the stable capacity and energy densities as cycling proceeds. Within the same charging/discharging voltage range (0.4 V−1.35 V in our case), as shown in Fig. 4(c), significant decreases in flow cell over-potential were observed as temperatures increased because of the enhanced electrolyte conductivity. Therefore, for a fixed charging upper-limit voltage, charging capacity improves as temperature increases (except at 40 °C). However, reactant crossover would improve simultaneously with increasing temperature, which results in reduced coulombic efficiency as the difference between charge capacity and discharge capacity increases as shown in Fig. 4(c). Consequently, a similar discharge capacity and decreasing discharge energy density occurs from room temperature to −5 °C, as plotted in Fig. 4(b). Moreover, at 40 °C, the cell exhibited a much reduced charge/discharge capacity as shown in Fig. 4(c), and also a significant capacity decay for the first few cycles accompanied by obvious electrolyte transfer from the positive side to the negative side, which was attributed to increasing diffusion of active species through membranes and thus severe crossover at elevated temperature. After 30 cycles at 40 °C, the electrolyte on both sides were subjected to ICP tests, from which nearly identical concentration values were obtained for vanadium and iron ions from both the positive and negative half cells, suggesting that the volume reduction at the positive side is the dominant factor contributing to capacity fading. Conversely, no apparent electrolyte volume change was observed during the cycling test at −5 °C and room temperature, leading to much improved capacity-retention capabilities. More detailed research on the capacity decay mechanism and optimization for the cells using porous separators is currently underway and will be reported in the future. Throughout the cycling tests carried out at −5 °C, room temperature, and 40 °C, no precipitation was observed. As a result, optimization of Fe/V system electrolytes successfully extended the lower temperature limit of the IVB operational temperature window to −5 °C, thus enabling IVBs to be deployed more widely around the world without the need for additional active heat management.

4. Conclusions

In this paper, we describe extensive matrix research undertaken to study the influence of temperature, compositions, and SOC on Fe/V RFBs electrolyte stability. Our research led to the identification of suitable electrolyte composition in terms of temperature stability. The most stable composition in the temperature range from −5 °C and 50 °C with the highest conductivity, which was composed of 1.5 M $FeCl_2$−1.5 M $VOSO_4$−3.0 M HCl, was used in flow battery electrochemical performance tests with commercial low-cost polyethylene microporous separators as the membranes. The flow cell exhibited stable cycling performance over the temperature range from −5 °C to 40 °C. The charge/discharge capacity remained stable over cycling at −5 °C and room temperature and exhibited an energy efficiency of 62% at −5 °C and 70% at room temperature. Capacity fading during the first few cycles at 40 °C was attributed to severe crossover of active species (vanadium and iron ions) across the microporous separator.

Acknowledgments

The authors would like to acknowledge financial support from the U.S. Department of Energy's (DOE's) Office of Electricity Delivery and Energy Reliability (OE) (under Contract No. 57558). We also are grateful for beneficial discussions with Dr. Imre Gyuk of the DOE-OE Grid Storage Program. Pacific Northwest National Laboratory is a multi-program national laboratory operated by Battelle for DOE under Contract DE-AC05-76RL01830.

References

[1] Z. Yang, J. Zhang, M.C.W. Kintner-Meyer, X. Lu, D. Choi, J.P. Lemmon, J. Liu, Chemical Reviews 111 (2011) 3577.
[2] W. Wang, Q. Luo, B. Li, X. Wei, L. Li, Z. Yang, Advanced Functional Materials (2012). http://dx.doi.org/10.1002/adfm.201200694.
[3] M. Skyllas-Kazacos, M.H. Chakrabarti, S.A. Hajimolana, F.S. Mjalli, M. Saleem, Journal of The Electrochemical Society 158 (2011) R55.
[4] S. Eckroad, Vanadium Redox Flow Batteries: An In-Depth Analysis, EPRI, Palo Alto, CA, 2007.
[5] C. Jia, J. Liu, C. Yan, Journal of Power Sources 195 (2010) 4380.
[6] C. Sun, J. Chen, H. Zhang, X. Han, Q. Luo, Journal of Power Sources 195 (2010) 890.
[7] M. Lopezatalaya, G. Codina, J.R. Perez, J.L. Vazquez, A. Aldaz, M.A. Climent, Journal of Power Sources 35 (1991) 225.
[8] M. Lopezatalaya, G. Codina, J.R. Perez, J.L. Vazquez, A. Aldaz, Journal of Power Sources 39 (1992) 147.
[9] W. Wang, S. Kim, B. Chen, Z. Nie, J. Zhang, G.-G. Xia, L. Li, Z. Yang, Energy & Environmental Science 4 (2011) 4068.
[10] W. Wang, Z. Nie, B. Chen, F. Chen, Q. Luo, X. Wei, G.-G. Xia, M. Skyllas-Kazacos, L. Li, Z. Yang, Advanced Energy Materials 2 (2012) 487.
[11] J. Mendham, Vogel's Quantitative Chemical Analysis, sixth ed., Prentice Hall, New York, 2000.
[12] J.A. Dean, Lange's Handbook of Chemistry, fifteenth ed., McGraw-Hill, 1999.
[13] X. Wei, L. Li, Q. Luo, Z. Nie, W. Wang, B. Li, G.-G. Xia, E. Miller, J. Chambers, Z. Yang, Journal of Power Sources 218 (2012) 39.